Supplementary Information

Aggrecan Nanoscale Solid-Fluid Interactions are a Primary Determinant of Cartilage Dynamic Mechanical Properties

Hadi T. Nia, Lin Han, Iman Soltani Bozchalooi, Peter Roughley, Kamal Youcef-Toumi, Alan J. Grodzinsky* and Christine Ortiz*

Endgrafting

Purified fetal bovine epiphyseal,[1] adult (38 years old) and newborn human aggrecan[2] aggrecan were chemically end-grafted to gold-coated planar substates (6 mm × 6 mm) as described previously.[3] Aggrecan was end-functionalized by reaction with 1μM dithiobis (sulfosuccinimidyl propionate) and 0.1mM dithiothreitol (Pierce) for 1hr. Excess reactants were removed by spinning (3500rpm, 6 hrs) with a centrifugal filter (Centricon, Millipore, 10kDa cutoff). Approximately 30μl of 1mg/ml modified aggrecan solution in deionized water was deposited onto freshly cleaned gold-coated surfaces and incubated for ~48hrs in a humidity chamber. Prior to nanomechanical measurements, the surfaces were thoroughly rinsed with deionized water.

Measurement of height, strain, stress

Aggrecan height was measured *versus* normal force using micro-contact printing and contact mode AFM imaging with probe of tip radius 22.5 μm (same as the one used in dynamic nanoindentation). Aggrecan was end-grafted within circular patterns (15 μm in diameter) and an OH-SAM filled the area outside of the circular area, as described previously.[3] The heights were measured in 0.001M–1M NaCl using ~0 – 1300 nN normal force (scan rate = 60μm/sec) and were averages of eight 30 μm line scans (256points/line).

High-frequency AFM-based nano-rheology system:

The complex dynamic modulus of cartilage was measured over a wide frequency range (1 Hz to 10 kHz), using a recently developed a high-frequency rheology system coupled to the commercial AFM, MFP-3D (Asylum Research, Santa Barbara, CA).[4] AFM-based micro/nano-

rheology of biological systems can be categorized into two main approaches: (I) Methods that probe the nanomechanical properties of the sample around the resonance frequency of the cantilevers, and (II) methods that probe the properties of the sample at a wide frequency band below any resonance frequencies of the apparatus, *e.g.*, those associated with the cantilever, driving piezo, base structure, etc. The former method is capable of measuring the mechanical response of the sample at ultra high frequencies, but is limited to obtaining narrowband frequency information from the sample.[5, 6] For the latter group,[7-9] a major obstacle is the limitation in the upper bound of the frequency range for which the sample excitation is free of any dynamics (*e.g.*, resonances).[10-12] The upper limit of the feasible excitation frequency range is mainly determined by the resonance frequency of the out of plane (vertical or z-) piezo and its supporting structure.[10, 12] To obtain a vertical displacement on the order of 10 micrometer in commercial AFMs, a large piezo (on the order of centimeters) needs to be chosen. As a result, the resonance frequency/bandwidth of the piezo is low,[13] resulting in an upper frequency limit of approximately 200 Hz[8] or as low as 10 Hz [9] in commercial AFMs. Our approach, which falls into the second category (wide-band rheology), is to couple a high-frequency actuating system to the commercial AFMs. The main component of the system is a small piezo, called the secondary piezo in this work (Figure S1). Unlike the z-piezo of the commercial AFM (called the 'primary piezo'), the secondary piezo is chosen to be small (2×2×2 mm) (Physik Instrumente, Auburn, MA) to maximize the feasible frequency range by pushing the resonance frequency of the combined piezo system to high frequencies. Unlike other AFM modifications in which the sample excitation is not free of dynamics of the apparatus (*e.g.*, resonances and load-dependent behavior), we made the displacement of the secondary piezo load-independent. We performed this by applying a permanent pre-stress to the piezo by clamping it between a beam and the

substrate. (An alternate solution that we tried is to add a mass that is significantly heavier than the sample's weight; this solution has the drawback of lowering the resonance frequency of the apparatus). The clamp system has its own mechanical resonances, which were diminished by optimizing the beam geometry and material. To have a low weight-to-stiffness ratio, we fashioned the beam from carbon fiber.

AFM tip specifications:

We used polystyrene colloidal probe tips gold coated with 100-nm thickness,, end radius, R ~ 22.5 μm, and 2.5 μm (Novascan, Ames, IA) attached to cantilevers with nominal spring constant k ~ 4.0 N/m.

Loading profile: Random Binary Sequence (RBS):

To identify the frequency response of a system, a stimulus is needed to excite the sample. A high power stimulus would lead to a high signal-to-noise ratio of the estimated frequency response. For a given maximum allowable excitation amplitude, a low crest factor is a preferred stimulus signal. In other words, for excitation signals of similar length, the one with a lower crest factor leads to more accurate estimated parameters (*i.e.* smaller variance). Crest factor, for a dataset, x[n], (n=1,…N), is defined as:

$$C = \sqrt{\frac{max_n x^2[n]}{\frac{1}{N}\sum_{n=1}^{N} x[n]^2}}$$

This index is minimized for a Random Binary Sequence (RBS) (crest factor of 1) where the excitation can only take two extreme values.[14, 15] As such, a RBS signal is preferred to

alternatives such as a swept sine of similar length (crest factor of $C \approx 1.4$). In addition, the random binary sequence data has the expected characteristics of wideband frequency content which would reveal the dynamics of the system under investigation *e.g.* Agrecan in this study.

To generate such a RBS signal, a sign operator (sign(x)=1 for $x \geq 0$ and sign(x)=-1 for $x < 0$) is applied to a set of simulated white Gaussian noise data, implemented in LabView (National Instrument Co., Austin, TX). The amplitude of the resulting dataset is then scaled to the maximum allowable excitation give to the secondary piezo actuator. To control the bandwidth of the resulting RBS signal, we applied a lowpass pass filter to the white Gaussian noise, prior to the application of the sign operator. In general, it is desired to have most of the excitation energy to be focused over the frequency range of interest for identification. For example, for a system where most of the important system information lies over the low frequency region, a lowpass filter with a sharp cutoff at relatively low frequencies should be applied to the generated white Gaussian signal prior to further processing. This step would limit the excitation of the system over the frequency ranges where the dynamics of the system is not of interest, or the actuators/sensors do not behave in a reliable manner.

The secondary piezo is then actuated by the resulting random binary sequence signal following an amplification step *via* a custom-made power amplifier. In this study, the sampling rate of the measurement was set to f_s = 100 kHz, the length of the time series was set to T = 20 s, and the cut-off frequency of the low pass filter was set at f_c = 10 Hz. The digital-to-analog conversions were performed by data acquisition system NI USB 6351 (National Instrument Co., Austin, TX).

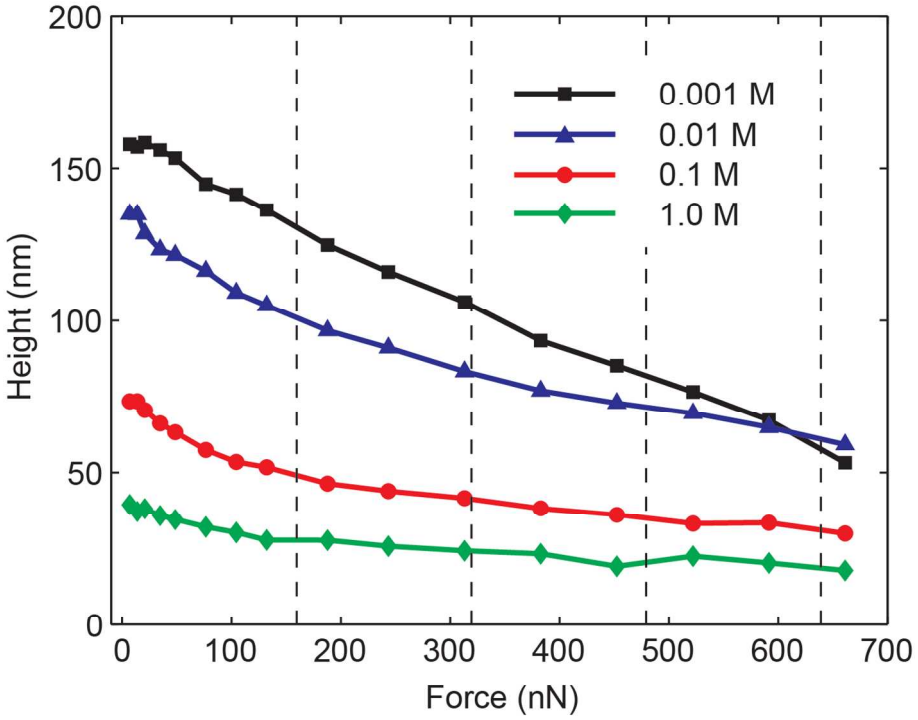

Figure S1. Height of newborn human aggrecan monolayer is measured *via* AFM in contact mode, as a function of the applied force. The measurement is performed in ionic strengths of 0.001 to 1.0 M NaCl.

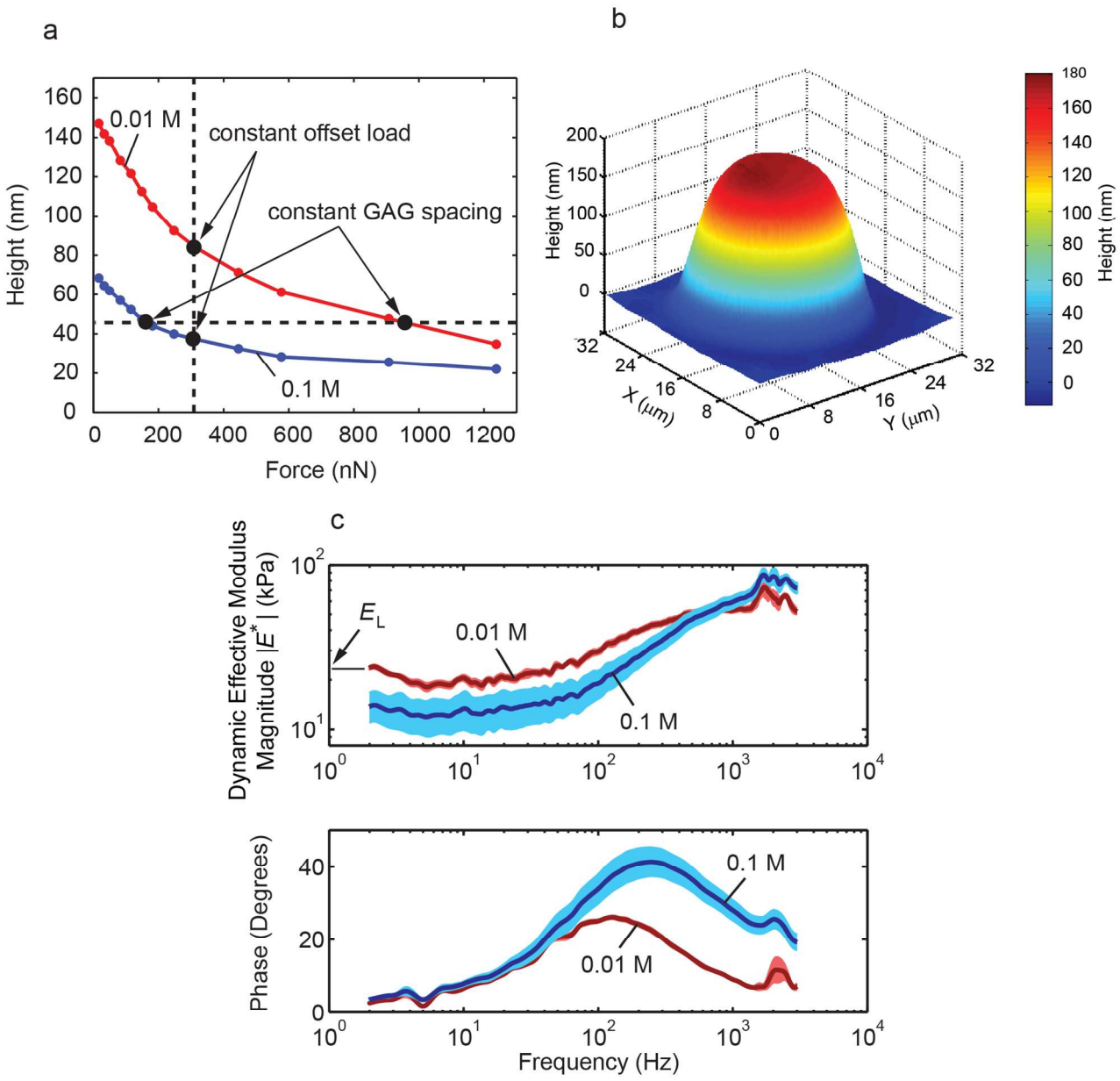

Figure S2 | The modulus of aggrecan monolayer is measured in displacement-control loading, representative of ECM response. (a) The height of aggrecan monolayer at 0.1 and 0.01 M is shown for both the displacement-control, and load-control measurements. **(b)** The aggrecan height is measured *via* micro-contact printing, followed by AFM imaging in contact mode at different ionic strengths and initial load on the AFM tip. **(c)** The modulus of aggrecan monolayer measured at displacement control is higher at lower ionic strength (0.01 M), which is consistent with macroscale experiments on ECM.[16] The displacement control is representative of what ECM feels when aggrecan goes under conformational changes *via* changes in ionic strength.

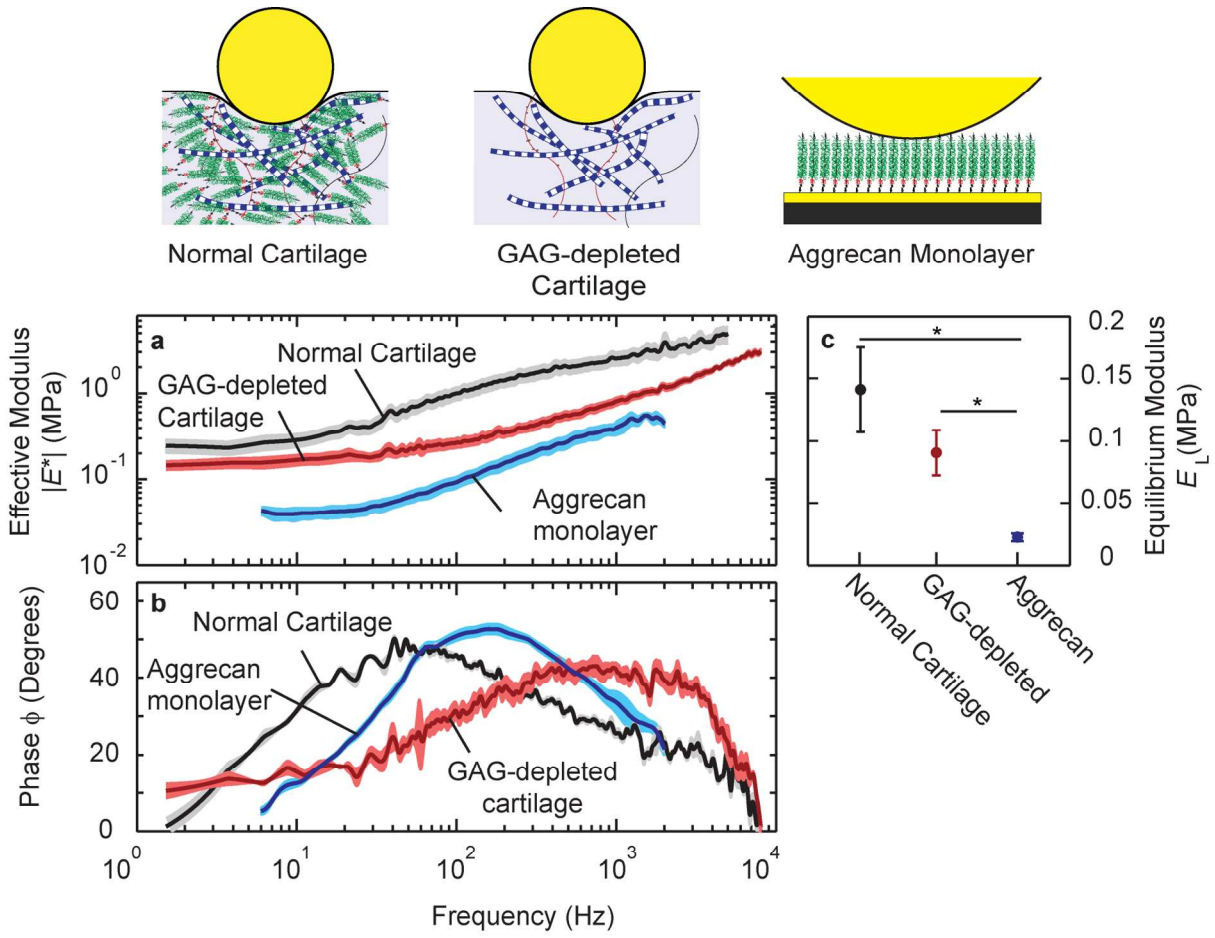

Figure S3 (a,b) The magnitude and phase of the dynamic modulus of fetal bovine aggrecan monolayer, normal and GAG-depleted newborn bovine cartilage matrix are measured and compared over the frequency range of 1Hz to 10kHz. **(c)** The equilibrium modulus, E_L, of these three systems are quantified and compared (*: $p<0.05$ using a t-test; data are mean ± SE). For normal and GAG-depleted cartilage, $N = 4$ animals, where E_L of each animal is the average over $M = 4$ plugs, and $m = 4$ different locations on each plug. For aggrecan, $N = 3$ plates, where for each plate, the k and E_L are averaged over $M = 6$ different locations.) Even though hydraulic permeabilities of the aggrecan monolayer and normal cartilage are similar, the peak frequencies of these two systems are different: from Eq. 1, the peak frequency depends on the Young's modulus and the contact distance between the AFM tip and the sample, in addition to the hydraulic permeability.

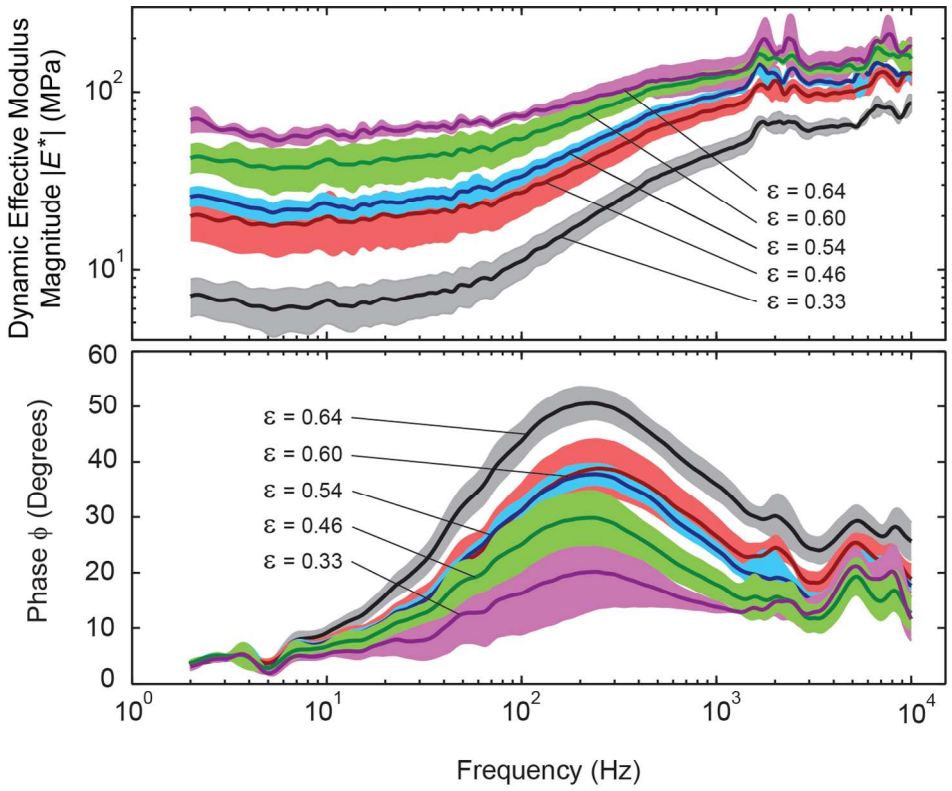

Figure S4 The variation in magnitude and phase of the dynamic modulus of the newborn human aggrecan layer are shown by changing the applied strain at a typical ionic strength of 0.1 M NaCl. The mean (solid line) and 95% confidence interval (shaded area) are based on $n = 6$ different locations on the substrate.

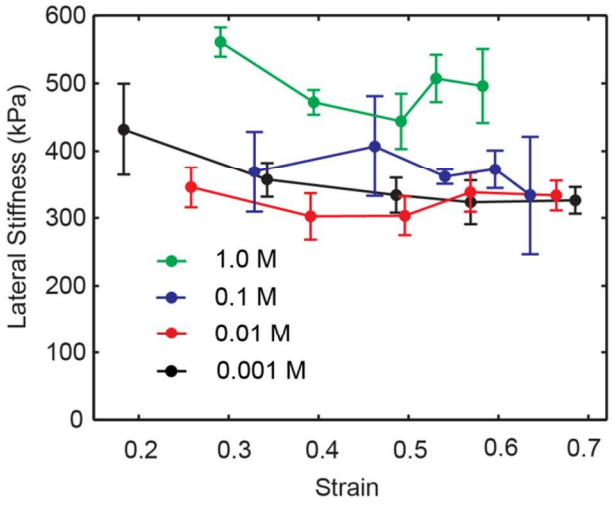

Figure S5 The lateral stiffness E_t of the newborn human aggrecan is estimated using the transversely isotropic finite element model at solutions with ionic strength of 0.001, 0.01, 0.1 and 1M under strain values in the range of 0.2 to 0.7. The data are reported as mean ±SE. (The values for E_a and k are shown in the main text).

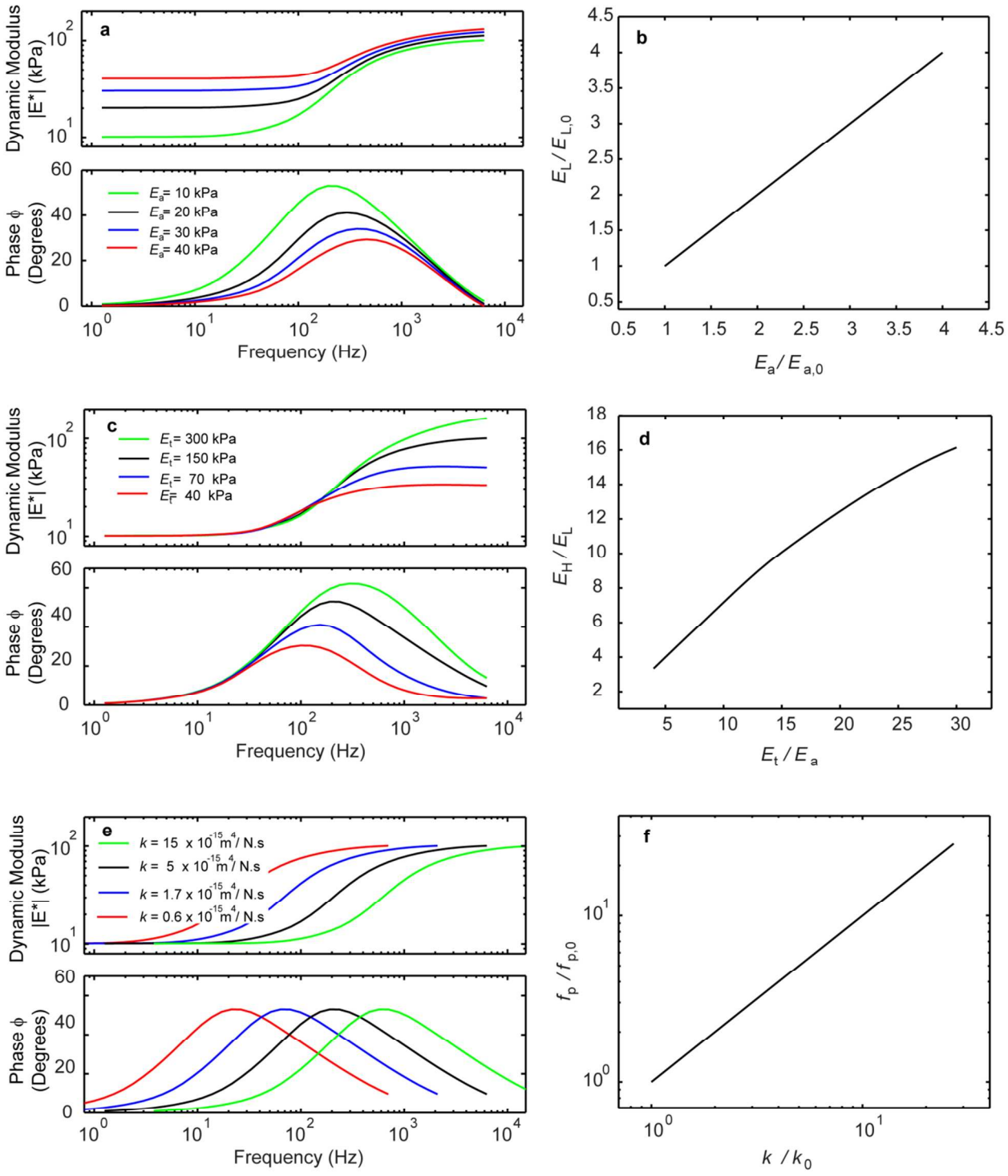

Figure S6 Parametric studies on the sensitivity of the model to values of axial equilibrium modulus E_a, transverse equilibrium modulus E_t and hydraulic permeability k. **(a, b)** The low-frequency modulus E_L changes linearly with axial modulus E_a when E_t and k are kept constant. **(a, b)** Varying E_t, when E_a and k are constant, results in an increase in E_H/E_L **(c,d)**, but no change in E_L. The peak frequency f_{peak} varies linearly with hydraulic permeabilty k. From this parametric study, we observe that the axial modulus is directly and linearly related to the low-frequency

modulus E_L, and the transverse modulus is related to the high-frequency modulus E_H through a weekly nonlinear relationship. This parametric study suggests why the transverse modulus does not vary much with depth. As shown in Fig. S4, even though the experimentally measured low frequency dynamic modulus changed by almost an order of magnitude, the high-frequency dynamic modulus didv not vary as much.

References:

1. Ng, L.; Grodzinsky, A. J.; Patwari, P.; Sandy, J.; Plaas, A.; Ortiz, C. Individual cartilage aggrecan macromolecules and their constituent glycosaminoglycans visualized *via* atomic force microscopy. *J. Struct. Biol.* 2003, 143, 242-257.
2. Lee, H.-Y.; Han, L.; Roughley, P.; Grodzinsky, A. J.; Ortiz, C. Age-related nanostructural and nanomechanical changes of individual human cartilage aggrecan monomers and their glycosaminoglycan side chains. *J. Struct. Biol.* 2012.
3. Dean, D.; Han, L.; Ortiz, C.; Grodzinsky, A. J. Nanoscale conformation and compressibility of cartilage aggrecan using microcontact printing and atomic force microscopy. *Macromolecules* 2005, 38, 4047-4049.
4. Nia, H. T.; Bozchalooi, I. S.; Li, Y.; Han, L.; Hung, H.-H.; Frank, E.; Youcef-Toumi, K.; Ortiz, C.; Grodzinsky, A. High-Bandwidth AFM-Based Rheology Reveals that Cartilage is Most Sensitive to High Loading Rates at Early Stages of Impairment. *Biophys. J.* 2013, 104, 1529-1537.
5. Gavara, N.; Chadwick, R. S. Noncontact microrheology at acoustic frequencies using frequency-modulated atomic force microscopy. *Nat. Methods* 7, 650-654.
6. Garcia, R.; Herruzo, E. T. The emergence of multifrequency force microscopy. *Nat. Nanotechnol.* 7, 217-226.
7. Han, L.; Frank, E. H.; Greene, J. J.; Lee, H. Y.; Hung, H. H. K.; Grodzinsky, A. J.; Ortiz, C. Time-dependent nanomechanics of cartilage. *Biophys. J.* 2011, 100, 1846-1854.
8. Nia, H. T.; Han, L.; Li, Y.; Ortiz, C.; Grodzinsky, A. Poroelasticity of Cartilage at the Nanoscale. *Biophys. J.* 2011, 101, 2304-2313.
9. Desrochers, J.; Amrein, M. A.; Matyas, J. R. Viscoelasticity of the articular cartilage surface in early osteoarthritis. *Osteoarthr. Cartil*., 2012, 20, 413-21.
10. Kodera, N.; Yamashita, H.; Ando, T. Active damping of the scanner for high-speed atomic force microscopy. *Rev. Sci. Instrum.* 2005, 76, 053708-053708-5.
11. Egawa, A.; Chiba, N.; Homma, K.; Chinone, K.; Muramatsu, H. High speed scanning by dual feedback control in SNOM/AFM. *J. Microsc.* 1999, 194, 325-328.
12. Bozchalooi, I. S.; Youcef-Toumi, K.; Burns, D. J.; Fantner, G. E. Compensator design for improved counterbalancing in high speed atomic force microscopy. *Rev. Sci. Instrum.* 82, 113712-113712-12.
13. Manalis, S. R.; Minne, S. C.; Quate, C. F. Atomic force microscopy for high speed imaging using cantilevers with an integrated actuator and sensor. *Appl. Phys. Lett.* 1996, 68, 871.
14. Ljung, L. *System identification*. Wiley Online Library: 1999.
15. Bozchalooi, I.; Youcef-Toumi, K.; Burns, D.; Fantner, G. Compensator design for improved counterbalancing in high speed atomic force microscopy. *Rev. Sci. Instrum.* 2011, 82, 113712-113712-12.

16. Buschmann, M. D.; Grodzinsky, A. J. A Molecular-Model of Proteoglycan-Associated Electrostatic Forces in Cartilage Mechanics. *J. Biomech. Eng.* 1995, 117, 179-192.